Civil Engineering and Applied Solutions

Research Article

journal homepage: ceas.journals.umz.ac.ir

CEAS Civil Engineering and Applied Solutions

Prediction of the Compressive Strength of Concrete Circular Columns Confined with FRP Using Neural Networks

Iman Dorosti [a], Ehasan Jahani [a*]

[a] *Department of Civil Engineering, Faculty of Engineering and Technology, University of Mazandaran, Babolsar, Iran*

ARTICLE INFO

Keywords:
Fiber-reinforced polymer (FRP)
Neural network
Confinement
High strength
Concrete columns

Article history:
Received 11 December 2025
Accepted 31 January 2026
Available online 01 July 2026

ABSTRACT

This study aims to predict the compressive strength of circular concrete columns confined with Fiber Reinforced Polymer (FRP), particularly for normal and high-strength concrete under axial loading. Existing predictive models have limitations, such as restricted applicability to specific ranges of concrete strength and the inability to account for FRP variations. To address these challenges, this research employs Neural Networks (NN) to enhance prediction accuracy and efficiency. A dataset of 574 data points was compiled from prior studies, encompassing various FRP types and concrete strengths. The NN models were trained using Levenberg-Marquardt (LM) and Bayesian Regularization (BR) methods, with different configurations tested to optimize performance. K-fold cross-validation was performed to ensure robustness. The models were validated and compared with existing approaches using R^2 and MSE as performance metrics. Results showed that the NN models achieved up to an 11.67% improvement in R^2 and an 84.24% reduction in MSE, significantly outperforming traditional methods. This study highlights the potential of NN-based approaches to provide reliable and accurate predictions for FRP-confined concrete columns. These findings offer valuable insights for engineers and designers, paving the way for safer and more efficient structural design practices in the construction industry.

Nomenclature

Aramid fiber reinforced polymer	AFRP
Artificial intelligence	AI
Bayesian Regularization	BR
Carbon fiber reinforced polymer	CFRP
Convolutional neural network	CNN
Deep neural network	DNN
Fiber reinforced polymer	FRP
Glass fiber reinforced polymer	GFRP
High modulus carbon fiber reinforced polymer	HM CFRP
Levenberg-Marquardt	LM
Life cycle assessment	LCA
Mean absolute percentage error	MAPE
Machine learning	ML
Mean squared error	MSE

* Corresponding author.
E-mail addresses: e.jahani@umz.ac.ir (E. Jahani).

https://doi.org/10.22080/ceas.2026.30756.1061
ISSN: 3092-7749/
How to cite this article: Dorosti, I., Jahani, E. Prediction of the Compressive Strength of Concrete Circular Columns Confined with FRP Using Neural Networks. Civil Engineering and Applied Solutions. 2025; 2(3): 28–44. doi:10.22080/ceas.2026.30756.1061.

Neural Network	NN
Near-surface mounted	NSM
Coefficient of determination	R^2
Radial basis function	RBF
Reinforced concrete	RC
Root mean squared error	RMSE
Support vector machine	SVM
Ultra-high modulus carbon fiber reinforced polymer	UHM CFRP

1. Introduction

In recent decades, the use of Fiber Reinforced Polymer (FRP) has increased significantly. One of the applications of FRP materials is in confining reinforced concrete columns, which increases compressive strength and ductility. The use of FRP has also been applied to high-strength and normal concrete [1-6], so guidelines for the use of these materials are needed [7]. On this basis, models for predicting the behavior of confined concrete columns have been presented. Most of these models were related to normal concrete, except for a limited number of models, such as those Mandal et al. [8], Cui and Sheikh [9], Berthet et al. [10] ,Xiao et al. [11], Girgin [12] and Raza et al. [13].

The comparison of the models presented so far with the experimental results shows that more accurate models are needed [14], as is a wider range of concrete compressive strength [7].

Since in recent years, the use of Neural Networks (NN) in various problems has increased significantly worldwide, the prediction of the compressive strength of this type of column can be done using artificial neural networks with an appropriate amount of data. These networks do not have the limitations of the experimental models presented and are more accurate. They also require much less cost and time than experimental models.

Farzinpour et al. [14] present a review paper that explores the methodologies and applications of Life Cycle Assessment (LCA) in the construction industry. It emphasizes the importance of LCA for sustainable decision-making, reviewing various studies on materials like cement, concrete, steel, and wood. The paper highlights recent advances in LCA, including circular economy principles and technological innovations, and discusses future directions such as data quality and standardization.

Naderpour et al. [15] presented an NN model for predicting the compressive strength of FRP-confined concrete using 213 data with an average prediction error of 9%, while the 3 models examined in this study had an average error of 13%.

In their study, Elsanadedy et al. [16] predicted the compressive strength and ultimate strain of FRP-confined concrete using NN and regression models. They considered 272 data for training and testing the NN. A sensitivity analysis was performed for the effective parameters of compressive strength and ultimate strain to introduce the regression model. The results of this study show that the use of NNs is both practical and useful for evaluating the compressive strength and ultimate strain of FRP-confined concrete.

Pham and Hadi [7] have compiled two data sets in a study. The first data set comprises 104 sample data points of rectangular concrete columns confined with FRP. The second data set includes 69 sample data points of square concrete columns also confined with FRP. They developed the NN model to predict the compressive strength and strain of this data and achieved an average absolute error of 5%.

Kumutha et al. [17] investigated the load-carrying capacity of reinforced concrete columns with Glass Fiber Reinforced Polymer (GFRP) using artificial intelligence (AI). 589 data were examined. The results of this study showed that the parameters of ultimate strength, ultimate strain, and spacing for longitudinal and transverse rebars are very important for predicting the load-bearing capacity of this type of column and the previous models did not take these parameters into account. They showed that among the AI methods used in this study, the Radial Basis Function (RBF) method had the highest accuracy and efficiency.

In their research, Koodiani et al. [18] used a method based on Machine Learning (ML) algorithms to develop design equations for the compressive strength of FRP-confined columns. The results of this research showed that the compressive strength limited to the elastic modulus of composite layers with a thickness of 2 mm was insensitive. A new equation was calibrated for specimens with a composite layer thickness greater than 2 mm, which provided very accurate estimates of the ultimate compressive strength for the experimental subset of this study.

In the study, Ali et al. [19] presented new models based on NN to predict the axial load capacities of concrete columns reinforced with FRP rebars. The axial load capacities of these columns were first predicted using the presented experimental models and then using Deep Neural Network (DNN) and Convolutional Neural Network (CNN) based models. The results show that the proposed DNN and CNN models predicted the axial load capacities of these types of columns with $R^2 = 0.943$ and $R^2 = 0.936$, respectively. In addition, the results showed that the proposed DNN and CNN models were more accurate than the experimental models with a reduction in Mean Absolute Percentage Error (MAPE) and Root Mean Squared Error (RMSE) by 52% and 42%, respectively.

In another study, Liang et al [20] investigated the prediction of residual fatigue life of composite sheets using vibration-based frequency measurements. In the study, NN, ML algorithms, and Support Vector Machine (SVM) were used to predict fatigue life. It was found that ML algorithms can effectively predict residual fatigue life by selecting an appropriate frequency. An inverse

algorithm based on SVM was introduced, which showed higher prediction accuracy with a limited data set.

Rasouli et al. [21] propose a new mix design method focusing on the durability of concrete by using supplementary cementitious materials and modified aggregate gradation. It evaluates the compressive strength, workability, and durability of various concrete mixes, achieving significant improvements in durability and strength. The paper develops a mix design process for optimized ratios of cement, aggregates, and SCMs, leading to durable and economical concrete mixes.

In a recent study, Ke et al. [22] investigated the shear strengthening of reinforced concrete (RC) beams using near-surface mounted (NSM) FRP bars/strips using ML techniques. They compiled a data set of 130 instances for rectangular and T-shaped beams characterized by 15 parameters. Their NN model used the Bayesian Regularization (BR) training method, which was further improved by a genetic algorithm. A comprehensive parametric analysis was performed to evaluate the influencing factors that affect the shear capacity of such beams. A design-oriented resistance model was then formulated and compared with existing models. The results showed that the newly proposed model outperformed the existing models in terms of accuracy.

In this study, in addition to normal circular concrete confined with FRP, circular concrete with high-strength FRP confinement was also investigated. Different types of NNs were investigated and finally, the best-performing NN from this investigation was compared with the previously proposed empirical models.

2. Existing experimental models

In this section, some models presented by researchers to predict the compressive strength of circular concrete columns confined with FRP are given. One of the most common forms for predicting compressive strength is as follows:

$$\frac{f'_{cc}}{f'_{co}} = 1 + k\left(\frac{f_l}{f'_{co}}\right)^n \tag{1}$$

where f'_{cc} is the compressive strength of confined concrete, f'_{co} is the compressive strength of unconfined concrete, k is the effective coefficient of confinement, f_l is the lateral confined pressure, and n is calibrated from a database. The relationship f_l is as follows:

$$f_l = \frac{2f_f t_f}{d} \tag{2}$$

where f_f is the tensile strength of FRP determined from flat coupon tests, t_f is the thickness of FRP, and d is the section diameter.

Some other researchers have also presented relationships with other forms. The models considered in this study for comparison with the NN are listed in Table 1.

Table 1. Models of compressive strength of circular columns.

Models	Equations
Richart et al. [23]	$\frac{f'_{cc}}{f'_{co}} = 1 + 4.1\frac{f_l}{f'_{co}}$
Mander et al. [24]	$\frac{f'_{cc}}{f'_{co}} = -1.254 + 2.254\sqrt{1 + \frac{7.94f_l}{f'_{co}}} - 2\frac{f_l}{f'_{co}}$
Mirmiran et al. [5]	$f'_{cc} = f'_{co} + 4.269(f_l)^{0.587}$
Samaan et al. [25]	$f'_{cc} = f'_{co} + 6(f_l)^{0.7}$
Razvi and Saatcioglu [26]	$f'_{cc} = f'_{co} + 6.7\,(f_l)^{0.83}$
Toutanji [27]	$\frac{f'_{cc}}{f'_{co}} = 1 + 3.5\left(\frac{f_l}{f'_{co}}\right)^{0.85}$
Spoelstra and Monti [28]	$f'_{cc} = f'_{co}\left(0.2 + 3\sqrt{\frac{f_l}{f'_{co}}}\right)$
Saafi et al. [29]	$\frac{f'_{cc}}{f'_{co}} = 1 + 2.2\left(\frac{f_l}{f'_{co}}\right)^{0.84}$
Shehata et al. [30]	$\frac{f'_{cc}}{f'_{co}} = 1 + 1.25\frac{f_l}{f'_{co}}$
Lam and Teng [31]	$\frac{f'_{cc}}{f'_{co}} = 1 + 3.3\frac{f_l}{f'_{co}}$
Campione and Miraglia [32]	$\frac{f'_{cc}}{f'_{co}} = 1 + 2\frac{f_l}{f'_{co}}$
Berthet et al. [10]	$\frac{f'_{cc}}{f'_{co}} = 1 + k\frac{f_l}{f'_{co}}, k = \begin{cases} 3.45 & (20 \le f'_{co}(MPa) \le 50) \\ \frac{9.5}{f'^{\frac{1}{4}}_{co}} & (50 \le f'_{co}(MPa) \le 200) \end{cases}$
Matthys et al. [33]	$\frac{f'_{cc}}{f'_{co}} = 1 + 2.3\left(\frac{f_l}{f'_{co}}\right)^{0.85}$
Kumutha et al. [17]	$\frac{f'_{cc}}{f'_{co}} = 1 + 0.93\frac{f_l}{f'_{co}}$
Wu et al. [34]	$\frac{f'_{cc}}{f'_{co}} = 1 + 3.2\frac{f_l}{f'_{co}}$

Wu and Zhou [35]	$\frac{f'_{cc}}{f'_{co}} = \frac{f_l}{f'_{co}} + \sqrt{\left(\frac{16.7}{(f'_{co})^{0.42}} - \frac{(f'_{co})^{0.42}}{16.7}\right)\frac{f_l}{f'_{co}} + 1}$
Yazici and Hadi [36]	$\frac{f'_{cc}}{f'_{co}} = 1 + 0.033K_N, K_N = \frac{2E_f t_f}{Df'_{co}}$ $(10 \le K_N \le 20)$
Pham and Hadi [7]	$f'_{cc} = 0.7f'_{co} + 1.8f_l + 5.7\frac{t}{d} + 13$
Girgin [12]	$\frac{f'_{cc}}{f'_{co}} = \left(1 + \frac{M}{B}\frac{f_l}{f'_{co}}\right)^B, B = 1 - 0.0172(\log f'_{co})^2$ $M = \begin{cases} 0.0035{f'_{co}}^2 - 0.056f'_{co} + 2.83 \ (7 \le f'_{co}(MPa) < 25) \\ 0.003{f'_{co}}^2 - 0.076f'_{co} + 5.46 \ (25 \le f'_{co}(MPa) < 108) \end{cases}$
Raza et al. [13]	$f'_{cc} = f'_{co} + 3f'_{co}\left(\frac{f_l}{f'_{co}}\right)^{\frac{3}{4}}$

The models presented for calculating f'_{cc} have their limitations and only a few models consider high-strength concrete in the range that can predict compressive strength. The relationship between f'_{cc} with f'_{co}, f_l, and k is so complicated that it is difficult to predict f'_{cc} by experimental methods due to the nonlinear behavior of concrete and FRP. Therefore, due to the need for a more accurate model, NNs were used in this study.

3. Neural networks

NNs have recently garnered significant attention. NNs are a branch of artificial intelligence inspired by the neural system of the brain. Similar to the brain, these NNs train by processing information and can be used for various applications.

NN consists of three layers: 1) the input layer, 2) the hidden layer, and 3) the output layer. In an NN, data are input into the input layer, and computations occur in the hidden layer (or layers). Finally, the NN generates predictions based on its training in the output layer. Each of these layers contains a certain number of neurons, which is determined based on the specific problem being investigated. However, in the hidden layer (or layers), the user has the flexibility to choose an appropriate number of neurons to achieve better results. In NNs, data are typically split into two or, in some cases, three groups based on the training method: 1) Train 2) Test 3) Validation. The data splitting ratio for NNs is determined based on various factors, such as the specific problem being investigated and the size of the dataset.

The process of training NNs proceeds as follows: First, we input the training data into the input layer. These inputs are then transmitted to the neurons in the hidden layers, each with distinct weights and biases. The output of these neurons is determined by an activation function specific to that hidden layer. Subsequently, this value is propagated to the neurons in the output layer, again with different weights and biases. Finally, in the output layer, the network's output is compared to the actual value from the training data to compute the error. The weights and biases of neurons across different layers are adjusted iteratively using selected training methods, with backpropagation being a common approach. The choice of activation functions in the hidden layer (or layers) depends on the specific problem being investigated.

In this study, two methods were used to train the neural network: 1) BR and 2) Levenberg-Marquardt (LM).

The BR training method had three training stop criteria to avoid overfitting and underfitting.

1) Epochs: This is the maximum number of epochs for which the training will stop if we reach this number.

2) Gradient: The minimum gradient value of the performance function that controls the changes in the performance function. If these changes are too small, the training stops.

3) Mu: initial value of learning to modify weights. If this number is large, the network will converge faster, and if it is small, the learning process will slow down. If the change in weights is less than this value, the training will be stopped.

In the LM training method, in addition to the above three stopping criteria, there is another criterion called Validation Checks. In this stop criterion, in each epoch, the performance function value is checked for validation data. If it is greater than that of the previous epoch, it is added to its counter. If this counter reaches the desired value, the training is stopped.

4. Experimental data

The data used in this study included 574 concrete specimens confined with FRP, which were taken from 58 studies conducted in the last few decades and collected by another researcher [7].

These data included various types of FRP, as follows:

- GFRP: 119 specimens
- Aramid Fiber-Reinforced Polymer (AFRP): 35 specimens
- AFRP tube: 23 specimens
- Carbon Fiber-Reinforced Polymer (CFRP): 317 specimens

- High Modulus CFRP (HM CFRP): 45 specimens
- Ultra-High Modulus CFRP (UHM CFRP): 7 specimens
- CFRP Tube: 28 specimens

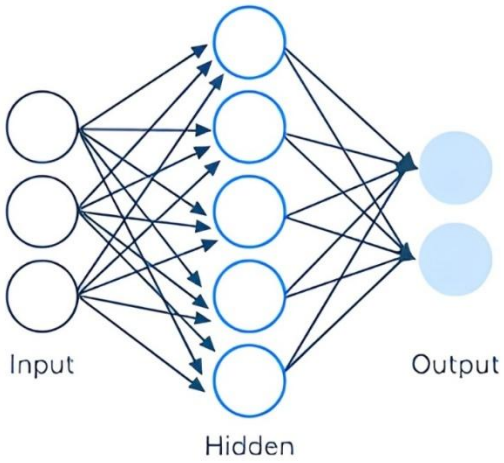

Fig. 1. Schematic of neural network.

The statistical properties of the data are shown in Table 2. The increase in compressive strength for data with confinement ranged from 10% to 440%. Specimens displaying a stress-strain curve with a descending branch and minimal strength increase were excluded from the database. In addition, specimens damaged due to premature rupture of FRP were excluded.

Table 2. Statistical properties of experimental data.

Parameter	d (mm)	h (mm)	f'_{co} (MPa)	E_f (GPa)	f_f (MPa)	t_f (mm)	f'_{cc} (MPa)
Maximum	406.40	812.80	169.7	640.00	4510.0	7.267	296.40
Minimum	51.00	102.00	15	18.47	237	0.110	37.23
Mean	156.64	315.13	49.43	180.55	2720.6	0.877	88.97
Standard deviation	56.62	114.24	24.05	117.82	1279.9	1.076	39.13
Coefficient of variation	0.36	0.36	0.49	0.65	0.47	1.227	0.44

5. Neural network modeling

For NN training as mentioned, 574 data were considered. 6 inputs were considered for the neural network, which are as follows:

- Diameter of section (d)
- Height of column (h)
- Compressive strength of unconfined concrete (f'_{co})
- FRP modulus of elasticity (E_f)
- FRP tensile strength (f_f)
- FRP thickness (t_f)

The output of this NN is f'_{cc}. Unlike experimental models that require predefined relationships for prediction, NN does not require any specific closed-form relationship. Instead of calculating f_l, effective variables in f_l were provided as input, enabling the NN to learn its relationship with f'_{cc} directly.

The Mean Squared Error (MSE) function and coefficient of determination (R^2) were used to calculate the prediction accuracy of the NNs and the presented models. The MSE relationship is as follows [37]:

$$MSE = \frac{1}{n}\sum_{i=1}^{n}(pre_i - exp_i)^2 \quad (3)$$

where n is the number of data, pre is the predicted value, and exp is the actual value obtained from the experiment. If the value of the MSE function is closer to 0, the prediction is more accurate.

R^2 quantifies the proportion of variation in the dependent variable (also known as the response variable) that can be attributed to the independent variables in a regression model. In simpler terms, it represents the percentage of variability in the dependent variable explained by the independent variables. The relationship of R^2 is as follows [38]:

$$R^2 = \left(\frac{n\sum xy - \sum x \sum y}{\sqrt{(\sum x^2 - (\sum x)^2) - (n\sum y - (\sum y)^2)}} \right)^2 \quad (4)$$

where n is the number of data, x and y are predicted and actual values, respectively. The closer the calculated value of R^2 is to 1, the higher the accuracy of the prediction.

The selected activation functions are the same for all NNs. The selected activation function in the hidden layers was sigmoid, and linear in the output layer. Because of the choice of the sigmoid as the activation function, the data were first normalized using Eq. 5.

$$x_{norm} = \frac{x - x_{min}}{x_{max} - x_{min}} \quad (5)$$

Epochs 2000 were considered, and the value of Validation checks was 10 for the LM training method. The results are shown in Tables 3 and 4.

According to the results obtained from the NNs, the best results were determined, as shown in Tables 2 and 3. In the LM training method, the NN performed best by splitting the data into 70, 15, and 15% for train, validation, and test, respectively. This NN included four hidden layers, with the number of neurons in each layer being 40, 40, 20, and 5. The results of this NN are shown in Figs. 2-5. The training process was stopped at epoch 25 because the validation checks reached the specified value. This NN had R^2 = 0.9839 and MSE = 0.000732, which was reached at epoch 15.

In the BR training method, the NN performed best by splitting the data into 80% and 20% for train and test, with two hidden layers and 15 and 5 neurons in each layer. This NN was stopped in epoch 1129 because of the gradient value in the NN performance function reached the allowed value. The value of this index for stopping in this type of NN was considered to be 10^{-7}. This NN with R^2 = 0.9902 and MSE = 0.000445 had the best prediction accuracy compared with other NNs using this training method.

5.1. Cross-validation using K-Fold method

Cross-validation is a robust statistical method used to evaluate and improve the performance of a predictive model. The technique is essential in ensuring that the model generalizes well to an independent dataset, thereby reducing overfitting and providing a more reliable measure of model performance. Among various cross-validation techniques, the K-Fold method is one of the most widely used due to its efficiency and comprehensiveness.

K-Fold Cross-Validation: In K-Fold Cross-Validation, the dataset is divided into 'K' equal-sized folds or subsets. The process follows these steps:

- Partitioning the Data: The entire dataset is randomly divided into K folds. Each fold is used exactly once as a validation dataset, while the K-1 remaining folds form the training dataset.
- Training and Validation: The model is trained on the training dataset (K-1 folds) and validated on the validation dataset (the remaining 1 fold). This step is repeated K times, with each fold being used exactly once as the validation data.
- Performance Aggregation: The performance of the model is evaluated using an appropriate metric (e.g., MSE, R^2) for each iteration. The K results are then averaged to provide a single estimation of the model's performance.

The major advantage of K-Fold Cross-Validation is that it ensures that every data point is used for both training and validation, providing a thorough evaluation of the model's ability to generalize. This method is particularly useful in small datasets where splitting the data into separate training and validation sets would result in limited training data.

Benefits:

- Reduced Overfitting: By training and validating the model on multiple folds, K-Fold Cross-Validation mitigates the risk of overfitting to a specific portion of the data.
- Better Utilization of Data: Every data point is used for both training and validation, maximizing the use of the dataset.
- Reliable Performance Metrics: Averaging the performance metrics across all folds provides a more stable and reliable estimate of the model's performance.

Choosing K: The choice of K is crucial for the effectiveness of the cross-validation. A common choice is K=10, which balances the bias-variance trade-off. Smaller values of K can lead to higher variance in the performance estimates, while larger values may result in higher computational costs.

In conclusion, K-Fold Cross-Validation is an indispensable tool for model evaluation and validation, providing comprehensive insights into the model's performance and ensuring its reliability in real-world applications.

The results of K-Fold Cross-Validation for the selected NNs are shown in Tables 5 and 6. The selected NNs were highlighted in Tables 3 and 4.

Table 3. Results of neural networks with the Levenberg-Marquardt training method.

Number of hidden layers	Number of neurons in hidden layers	Train, validation, and test ratio	R^2				MSE			
			Train	Validation	Test	All	Train	Validation	Test	All
1	5	70% 15% 15%	0.967014	0.957462	0.954914	0.963986	0.001484	0.002128	0.001681	0.001610
	10		0.972176	0.968095	0.968661	0.971136	0.001217	0.001415	0.001538	0.001295
	20		0.978462	0.968850	0.970540	0.976461	0.001030	0.000923	0.001328	0.001059
	40		0.980457	0.951088	0.963552	0.973849	0.000906	0.002238	0.001378	0.001176
2	5 5		0.973375	0.956683	0.960703	0.969555	0.001263	0.001436	0.001768	0.001365
	10 10		0.981378	0.970759	0.958945	0.976836	0.000854	0.001293	0.001676	0.001043
	20 20		0.986742	0.962981	0.962032	0.979930	0.000622	0.001538	0.001659	0.000915
	40 40		0.983481	0.968584	0.972264	0.978708	0.000802	0.001568	0.001243	0.000983
3	5 5 5		0.970681	0.973464	0.969890	0.970600	0.001254	0.001650	0.001315	0.001323
	10 10 10		0.977660	0.958927	0.961406	0.973236	0.001071	0.001642	0.001380	0.001203
	20 20 20		0.985897	0.976323	0.973453	0.982315	0.000626	0.001290	0.001133	0.000801
	40 40 40		0.989365	0.936055	0.920921	0.971385	0.000490	0.002942	0.003510	0.001310
4	5 5 5 5		0.974805	0.965200	0.965296	0.971481	0.001061	0.001672	0.001922	0.001282
	10 10 10 10		0.982719	0.963263	0.944529	0.976352	0.000887	0.001418	0.001549	0.001066
	20 20 20 20		0.981651	0.973809	0.971193	0.978088	0.000747	0.001511	0.001614	0.000991
	40 40 20 5		0.988577	0.969366	0.970979	0.983940	0.000558	0.001099	0.001176	0.000732
1	5	60% 20% 20%	0.968806	0.958553	0.951597	0.964021	0.001522	0.001654	0.001830	0.001610
	10		0.980082	0.967028	0.956950	0.973872	0.000982	0.001615	0.001335	0.001180
	20		0.979269	0.940721	0.959092	0.969526	0.001039	0.001983	0.001790	0.001379
	40		0.982244	0.950036	0.961463	0.973363	0.000917	0.001615	0.001613	0.001196
2	5 5		0.971677	0.964895	0.945492	0.966982	0.001381	0.001821	0.001440	0.001481
	10 10		0.977850	0.968667	0.961413	0.973018	0.001051	0.001398	0.001571	0.001225
	20 20		0.976455	0.958481	0.972956	0.971907	0.001089	0.001756	0.001463	0.001298
	40 40		0.992031	0.944389	0.960900	0.977819	0.000391	0.002324	0.001499	0.001000
3	5 5 5		0.972904	0.965232	0.949763	0.967846	0.001416	0.001464	0.001589	0.001460
	10 10 10		0.979569	0.965853	0.958218	0.973244	0.000952	0.001670	0.001482	0.001202
	20 20 20		0.988670	0.966814	0.966871	0.979423	0.000509	0.001709	0.001422	0.000932
	40 40 40		0.985083	0.953356	0.966123	0.978117	0.000799	0.000963	0.001627	0.000997
4	5 5 5 5		0.970233	0.908527	0.970269	0.960213	0.001292	0.003259	0.001754	0.001779
	10 10 10 10		0.981371	0.961754	0.968427	0.975011	0.000853	0.001625	0.001438	0.001125
	20 20 20 20		0.989925	0.969365	0.963427	0.982285	0.000523	0.001265	0.001190	0.000805
	40 40 20 5		0.991493	0.974233	0.952760	0.982504	0.000425	0.001198	0.001469	0.000789

Table 4. Results of neural networks with the Bayesian regularization training method.

Number of hidden layers	Number of neurons in layers	Train and test ratio	R^2			MSE		
			Train	Test	All	Train	Test	All
1	5	80% 20%	0.970942	0.960350	0.969464	0.001337	0.001515	0.001368
	10		0.981475	0.964940	0.978443	0.000841	0.001597	0.000972
	15		0.985428	0.970538	0.983783	0.000698	0.000893	0.000732
	20		0.984546	0.978377	0.983569	0.000710	0.000894	0.000742
2	5 5		0.980808	0.979823	0.979823	0.000869	0.001108	0.000911
	10 5		0.988818	0.952899	0.984772	0.000546	0.001371	0.000690
	10 10		0.993728	0.965076	0.987631	0.000272	0.001932	0.000561
	15 5		0.993210	0.977448	0.990197	0.000304	0.001112	0.000445
	20 5		0.995284	0.947688	0.986940	0.000213	0.002381	0.000591
3	5 5 5		0.983419	0.983453	0.983399	0.000692	0.001031	0.000751
	10 10 5		0.996650	0.943088	0.987337	0.000155	0.002607	0.000582
	10 10 10		0.996846	0.939862	0.988004	0.000147	0.002435	0.000546

	15 5 5		0.996144	0.902602	0.980057	0.000177	0.004378	0.000909
	15 10 5		0.996755	0.890705	0.976145	0.000146	0.005595	0.001095
1	5		0.973334	0.960750	0.969666	0.001182	0.001878	0.001364
	10		0.980359	0.962019	0.975896	0.000908	0.001582	0.001084
	15		0.987316	0.960083	0.982650	0.000632	0.001213	0.000784
	20		0.989116	0.949085	0.980084	0.000517	0.001982	0.000900
2	5 5	70% 30%	0.979644	0.978451	0.979261	0.000918	0.000985	0.000936
	10 5		0.987445	0.956709	0.980436	0.000589	0.001709	0.000882
	10 10		0.994192	0.966829	0.986166	0.000252	0.001690	0.000628
	15 5		0.993178	0.969857	0.986380	0.000298	0.001522	0.000618
	20 5		0.996594	0.891537	0.975327	0.000166	0.003795	0.001114
3	5 5 5		0.987914	0.964608	0.982041	0.000558	0.001532	0.000813
	10 10 5		0.996904	0.957678	0.986789	0.000142	0.001905	0.000603
	10 10 10		0.997488	0.958904	0.987187	0.000115	0.001925	0.000588
	15 5 5		0.995895	0.937744	0.981013	0.000187	0.002763	0.000860
	15 10 5		0.996903	0.944023	0.979052	0.000130	0.003365	0.000975

Table 5. K-fold cross-validation for the Levenberg-Marquardt method.

K	R^2				MSE			
	Train	Validation	Test	All	Train	Validation	Test	All
1	0.9580	0.9554	0.9533	0.9569	0.00197	0.003401	0.001801	0.0022
2	0.9711	0.9624	0.9633	0.9686	0.00126	0.001403	0.00216	0.0014
3	0.9785	0.9777	0.9402	0.9726	0.00099	0.001048	0.002049	0.0012
4	0.9691	0.9476	0.9354	0.9608	0.00136	0.001681	0.003588	0.0017
5	0.9750	0.9627	0.9312	0.9666	0.00111	0.000987	0.003316	0.0014
6	0.9686	0.9602	0.9639	0.9666	0.00148	0.001773	0.001074	0.0015
7	0.9705	0.9588	0.9775	0.9698	0.00131	0.002319	0.001191	0.0014
8	0.9837	0.9438	0.9464	0.9721	0.00072	0.002169	0.002837	0.0013
9	0.9727	0.9671	0.9575	0.9696	0.00125	0.001288	0.001578	0.0013
10	0.9555	0.9056	0.9526	0.9476	0.00198	0.006185	0.002251	0.0027
Average	0.9703	0.9541	0.9521	0.9651	0.001343	0.002225	0.002185	0.001610

Table 6. K-fold cross-validation for the Bayesian regularization method.

K	R^2			MSE		
	Train	Test	All	Train	Test	All
1	0.9833	0.9669	0.9800	0.000748	0.001684	0.000935
2	0.9867	0.9571	0.9808	0.000603	0.002298	0.000942
3	0.9871	0.9538	0.9804	0.000594	0.001939	0.000863
4	0.9733	0.9590	0.9705	0.001269	0.001655	0.001346
5	0.9574	0.9705	0.9600	0.002123	0.000861	0.00187
6	0.9792	0.9775	0.9789	0.000956	0.000922	0.000949
7	0.9772	0.9643	0.9747	0.001042	0.002202	0.001274
8	0.9526	0.9832	0.9587	0.002495	0.001125	0.002221
9	0.9848	0.9704	0.9819	0.000693	0.00252	0.001058
10	0.9599	0.9560	0.9591	0.001824	0.00229	0.001917
Average	0.9742	0.9659	0.9725	0.001235	0.00175	0.001338

Tables 5 and 6 summarize the K-fold cross-validation results for the neural network models trained using LM and BR methods, respectively. Both tables present R^2 and Mean Squared Error (MSE) values for training, validation, test, and overall datasets, showing high R^2 (0.9476 to 0.9819) and low MSE (0.00072 to 0.0027) values. These results indicate the robustness and superior predictive accuracy of the neural network models, with the BR method showing slightly better performance on average.

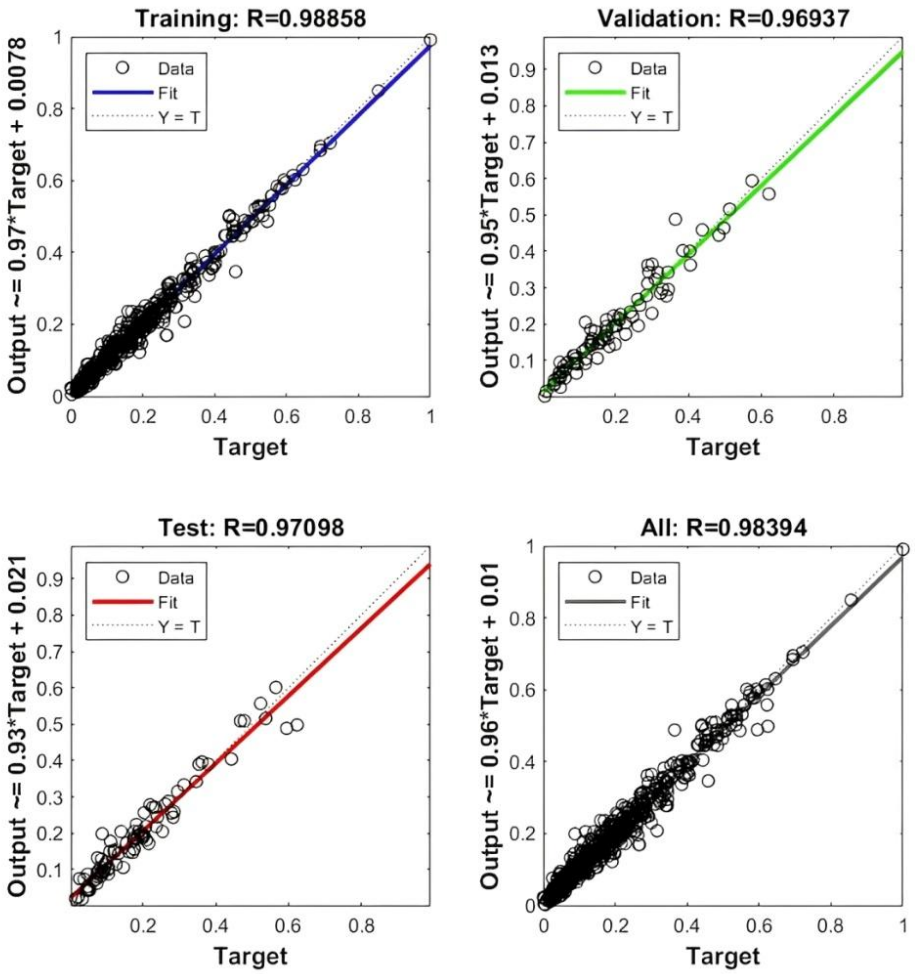

Fig. 2. Training regression of the proposed neural network with levenberg-marquardt training method.

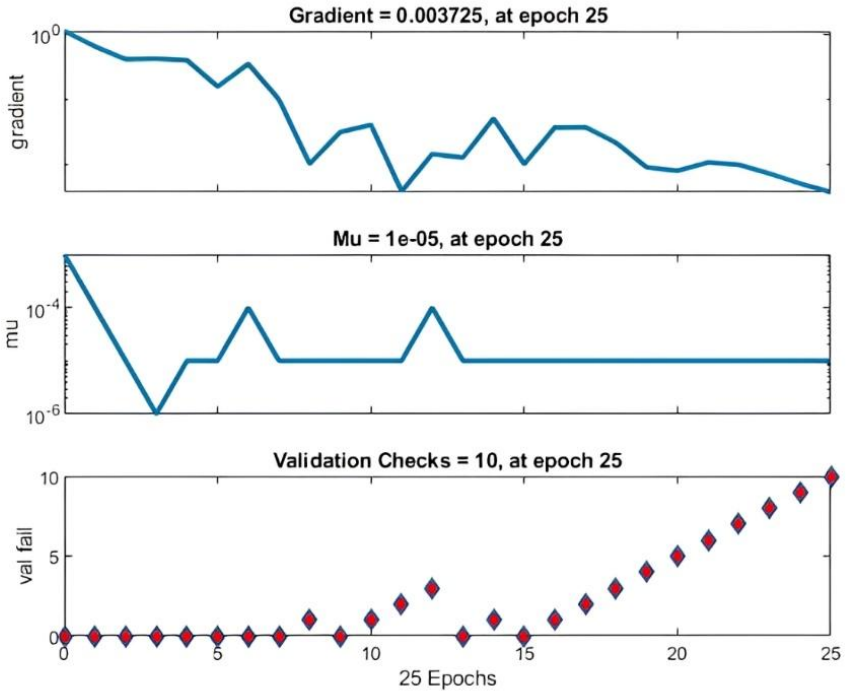

Fig. 3. Training state of the proposed neural network with levenberg-marquardt training method.

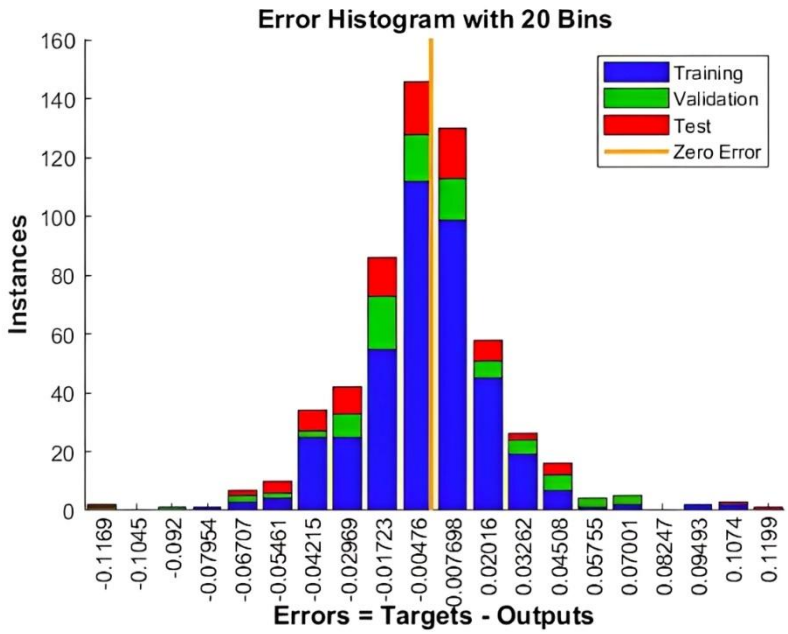

Fig. 4. Error histogram of the proposed neural network with levenberg-marquardt training method.

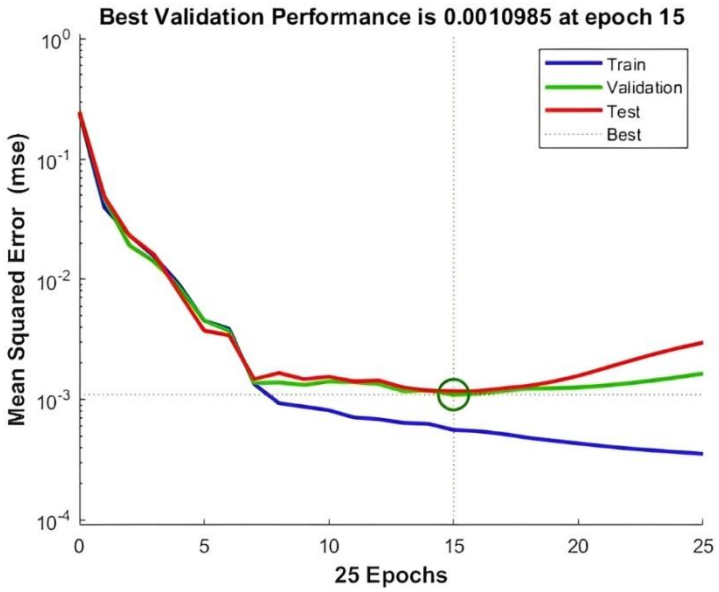

Fig. 5. Training performance of the proposed neural network with levenberg-marquardt training method.

Table 7 provides an extensive quantitative comparison between a wide range of conventional analytical and semi-empirical models and the proposed artificial neural network (ANN) models for predicting the axial behavior of FRP-confined concrete columns. The evaluation is conducted using the coefficient of determination (R^2) and mean squared error (MSE), which together offer a robust measure of both goodness-of-fit and prediction accuracy.

The traditional models demonstrate varying levels of predictive capability, with R^2 values ranging from as low as 0.7501 to a maximum of approximately 0.8889 [5, 26]. This spread indicates a significant inconsistency in the ability of classical formulations to accurately represent the complex confinement mechanisms of FRP systems. Furthermore, although some models exhibit relatively high R^2 values, they are often accompanied by comparatively large MSE values, suggesting that a good overall correlation does not necessarily translate into precise point-wise predictions.

A closer examination reveals that earlier models, such as those proposed by Richart et al. and Mander et al., which were originally developed for steel-confined concrete, show noticeably inferior performance when applied to FRP-confined systems. Their higher MSE values reflect the limitations of extending steel-based confinement assumptions to FRP materials, which exhibit fundamentally different stress–strain behavior and failure mechanisms. More recent formulations, including those by Wu and Zhou [35], Campione and Campione and Miraglia [32], and Pham and Hadi [7], demonstrate improved accuracy due to the incorporation of FRP-specific parameters; however, their predictive performance still remains substantially below that of the ANN models.

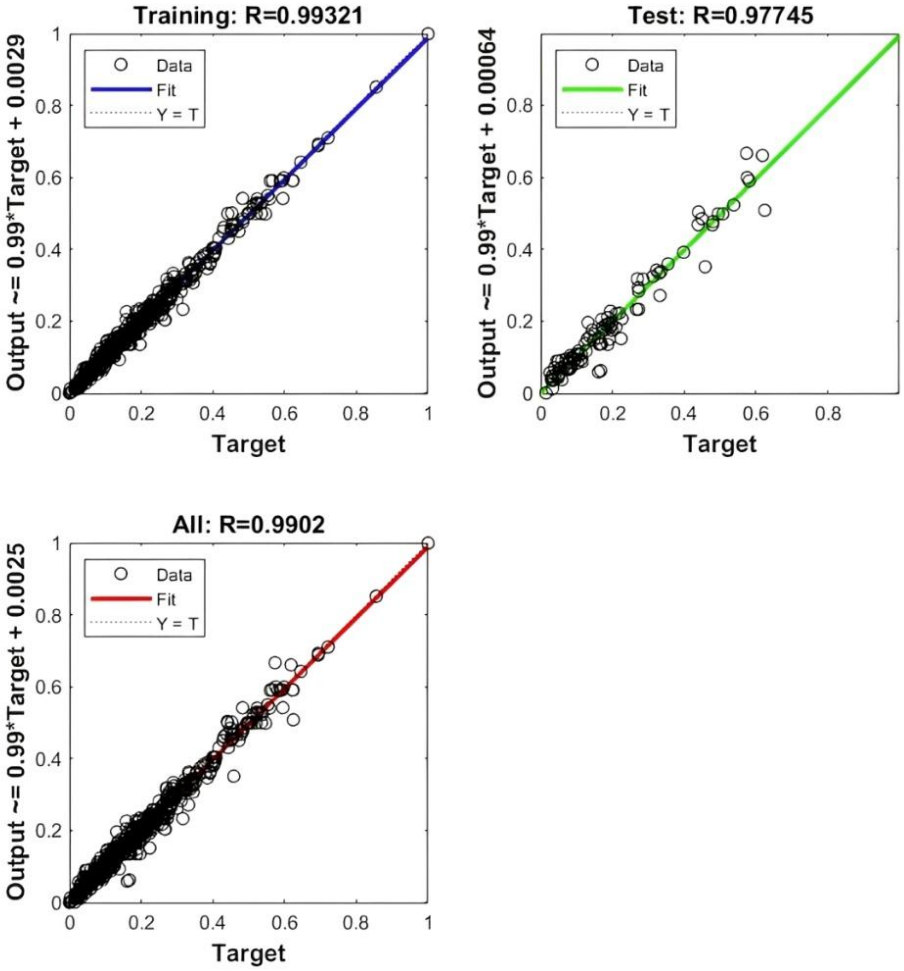

Fig. 6. Training regression of the proposed neural network using the Bayesian regularization training method.

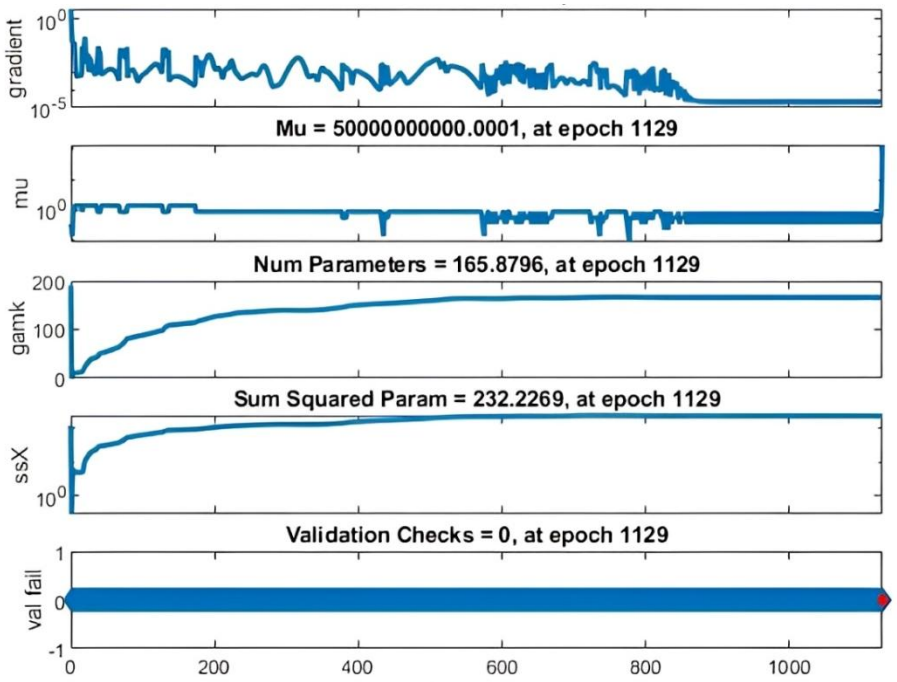

Fig. 7. Training state of the proposed neural network with the Bayesian regularization training method.

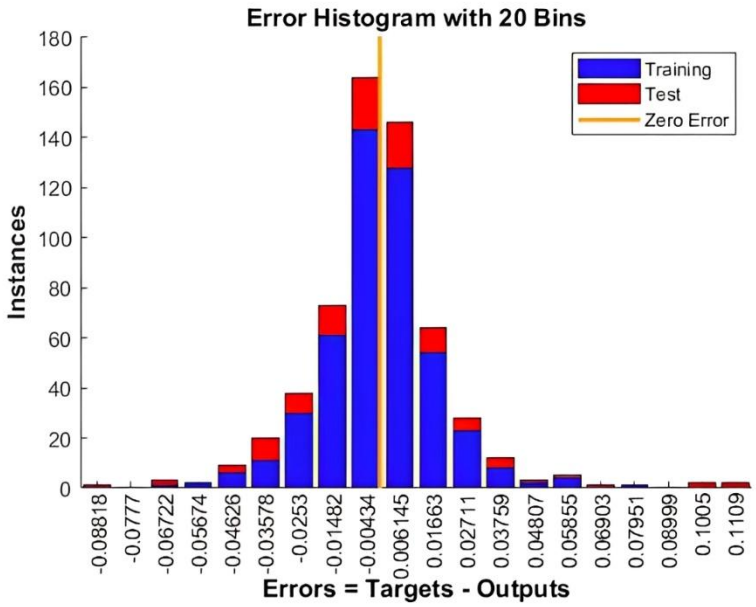

Fig. 8. Error histogram of the proposed neural network with the Bayesian regularization training method.

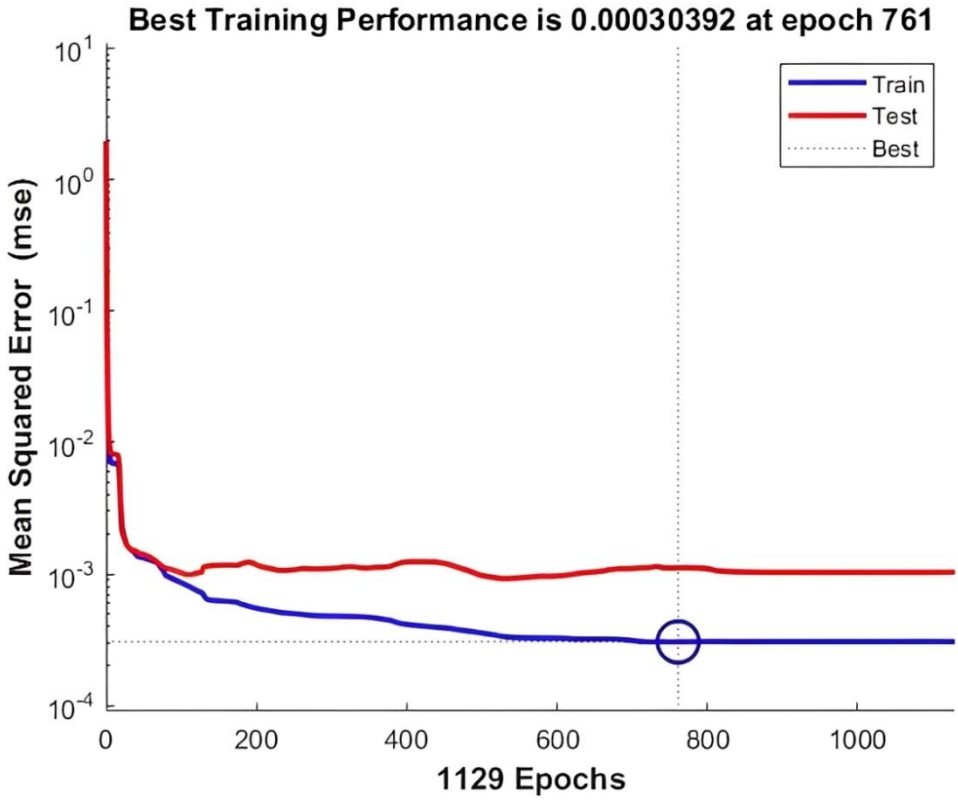

Fig. 9. Training performance of the proposed neural network with the Bayesian regularization training method.

Table 7. Comparison of the presented models with the proposed neural networks.

Models	R^2	MSE
Richart et al. [23]	0.8746	0.045365
Mander et al. [24]	0.8027	0.027231
Mirmiran et al. [5]	0.7501	0.009875
Samaan et al. [25]	0.8659	0.003849
Razvi and Saatcioglu [26]	0.8889	0.030834
Toutanji [27]	0.8851	0.035536

Spoelstra and Monti [28]	0.8584	0.007468
Saafi et al. [29]	0.8693	0.006327
Shehata et al. [30]	0.8404	0.006924
Lam and Teng [31]	0.8835	0.020448
Campione and Miraglia [32]	0.8803	0.003473
Berthet et al. [10]	0.8756	0.019586
Matthys et al. [33]	0.8732	0.007181
Kumutha et al. [17]	0.8014	0.011346
Wu et al. [34]	0.8843	0.018108
Wu and Zhou [35]	0.8867	0.002823
Yazici and Hadi [36]	0.7949	0.007724
Pham and Hadi [7]	0.8868	0.003099
Girgin [12]	0.8679	0.004365
Raza et al [13]	0.8721	0.026727
Neural Network (Levenberg- Marquardt)	0.9839	0.000732
Neural Network (Bayesian Regularization)	0.9902	0.000445

In contrast, the ANN models significantly outperform all conventional approaches. The Levenberg–Marquardt (LM) neural network achieves an R^2 value of 0.9839, which corresponds to an improvement of approximately 10–23% over most traditional models. More importantly, its MSE is reduced by nearly one to two orders of magnitude, highlighting a dramatic decrease in prediction error. This improvement confirms the superior capability of ANNs in capturing nonlinear interactions among material properties, geometric parameters, and confinement effects that are difficult to express through closed-form equations.

The Bayesian Regularization (BR) neural network exhibits the best overall performance, achieving the highest R^2 (0.9902) and the lowest MSE (0.000445) among all evaluated models. When compared to the best-performing conventional model, the BR approach reduces the MSE by more than 85–90%, demonstrating its enhanced generalization ability. This improvement can be attributed to the inherent regularization mechanism of the BR algorithm, which effectively controls overfitting and ensures stable performance across a wide range of input conditions.

Overall, the comparative results clearly indicate that while conventional models can provide approximate estimates of axial behavior, they are limited by simplifying assumptions and restricted applicability ranges. In contrast, ANN-based models, particularly those trained using Bayesian Regularization, offer a highly accurate, reliable, and flexible predictive framework. These findings strongly support the adoption of artificial intelligence techniques for modeling the complex mechanical response of FRP-confined reinforced concrete columns and highlight their potential to replace or complement traditional analytical formulations in advanced structural design and assessment.

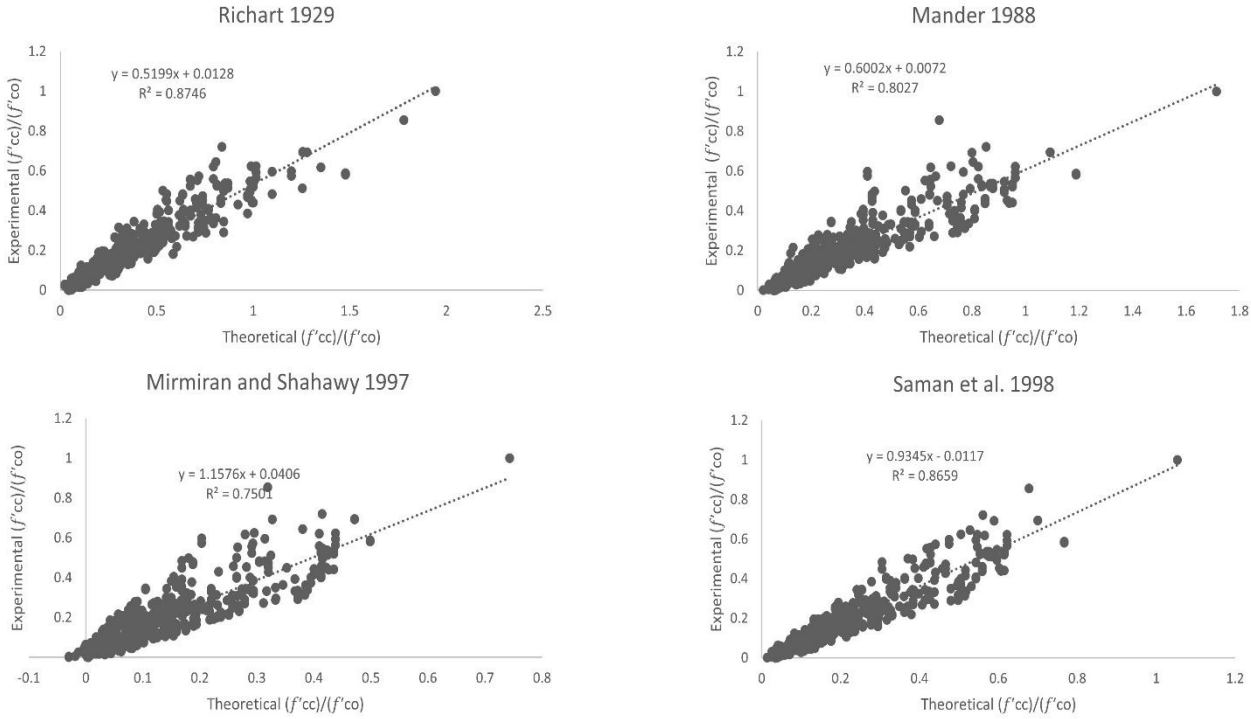

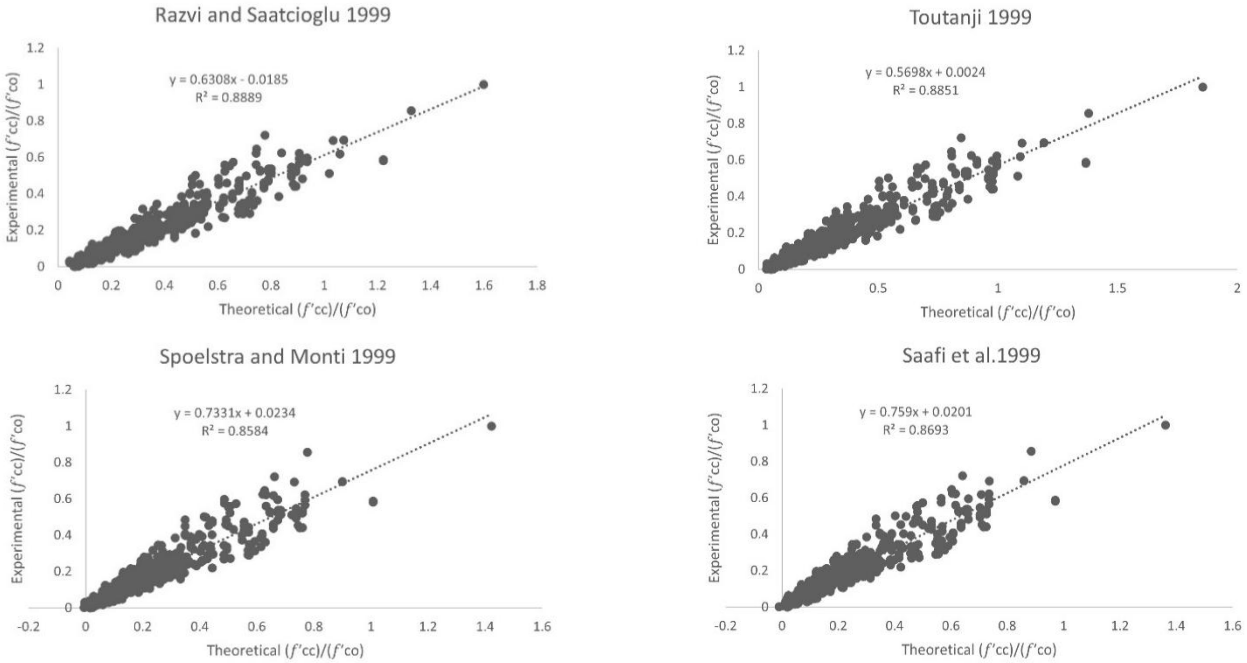

Fig. 10. Regression diagram of the presented models.

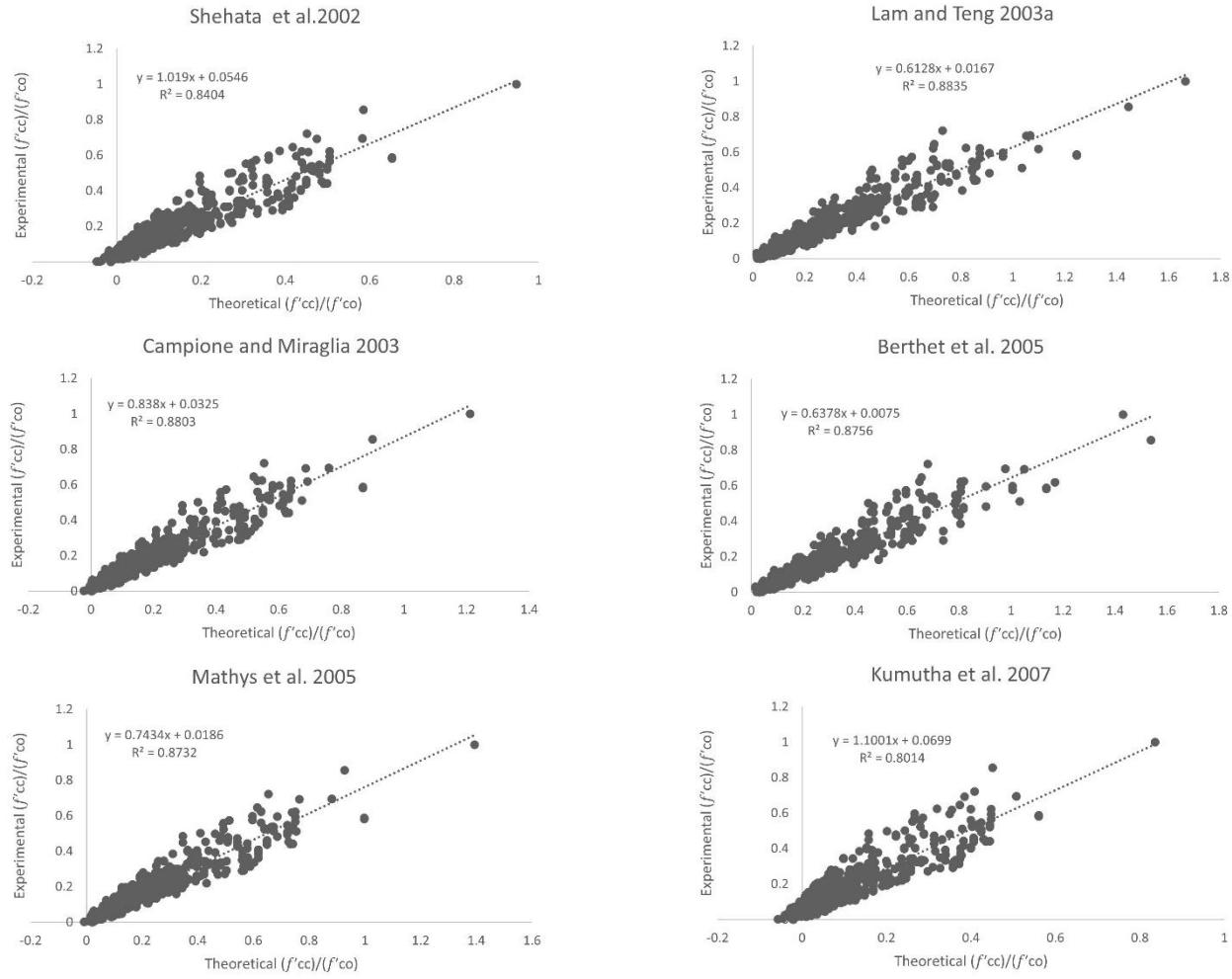

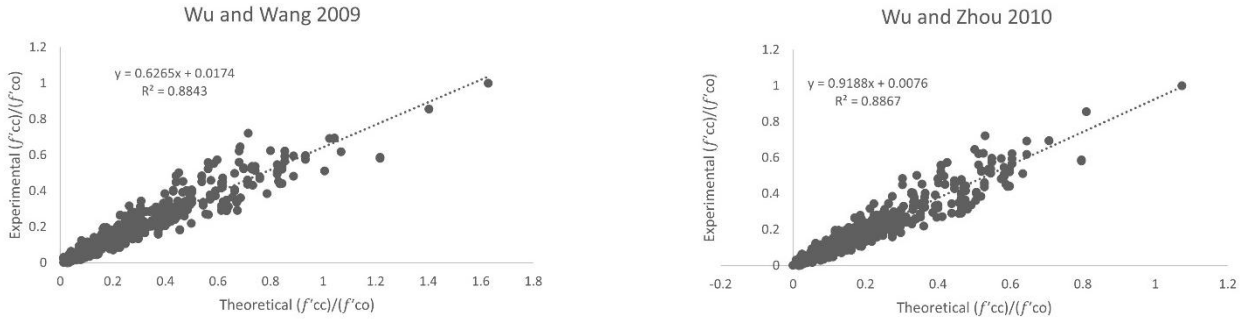

Fig. 11. Regression diagram of the presented models.

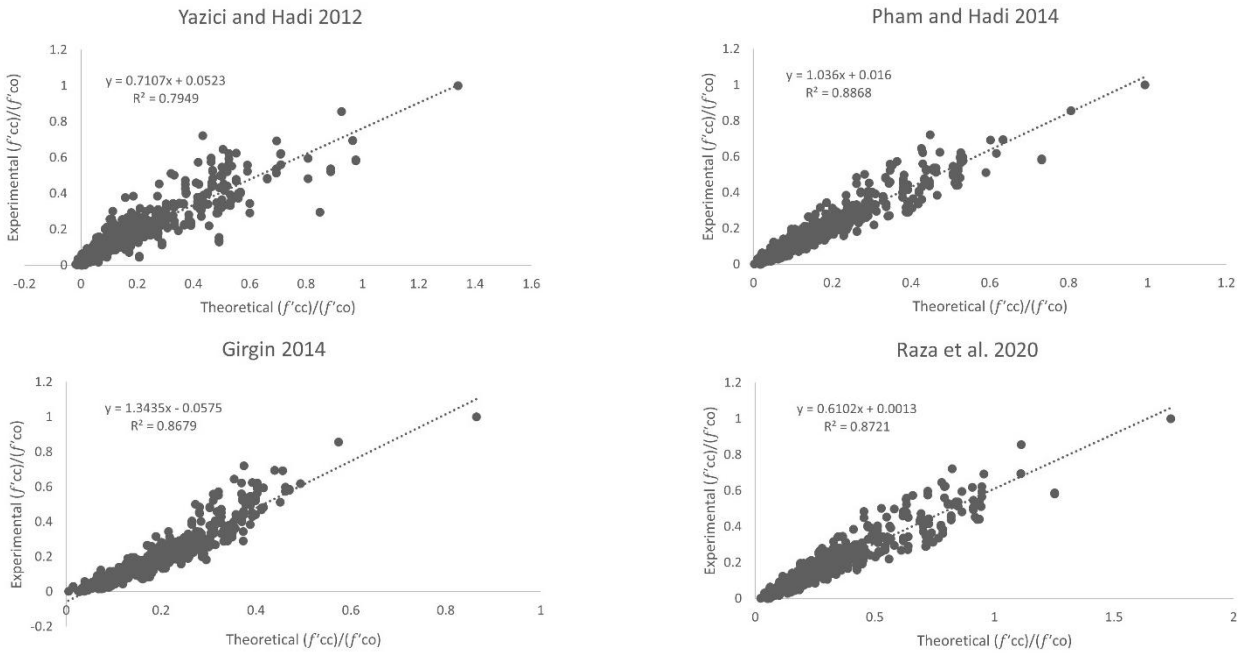

Fig. 12. Regression diagram of the presented models.

6. Conclusion

With the growing use of FRP in structural applications, accurately predicting their behavior has become increasingly critical. However, existing models for estimating the compressive strength of FRP-confined circular concrete columns have notable limitations, such as restricted applicability to specific ranges of f'_{co} and a lack of consideration for different FRP types. To address these limitations, this study introduced a neural network (NN) approach to predict the compressive strength of normal to high-strength FRP-confined concrete columns.

A diverse dataset, including various FRP types, was compiled from prior research to train the NN. Two training methods, Levenberg-Marquardt (LM) and Bayesian Regularization (BR), were implemented, and multiple configurations of hidden layers and neurons were tested. K-fold cross-validation was performed to ensure the robustness of the models. The two most effective NN models were identified and compared with existing models using R^2 and MSE as performance metrics. The findings demonstrated that the NN models outperformed traditional models, achieving up to an 11.67% improvement in R^2 and an 84.24% reduction in MSE.

These results confirm the superior accuracy and potential of NNs in providing robust predictions for FRP-confined concrete columns, offering a reliable alternative to conventional methods. The use of K-fold cross-validation further reinforces the reliability and generalizability of the proposed models.

Statements & Declarations

Author contributions

Iman Dorosti: Investigation, Formal analysis, Validation, Resources, Writing - Original Draft, Writing - Review & Editing.

Ehsan Jahani: Conceptualization, Methodology, Project administration, Supervision, Writing - Review & Editing.

Funding

The authors received no financial support for the research, authorship, and/or publication of this article.

Data availability

The data presented in this study will be available upon request from the corresponding author.

Declarations

The authors declare no conflict of interest.

References

[1] Hadi, M. Behaviour of FRP wrapped normal strength concrete columns under eccentric loading. Composite structures, 2006; 72: 503-511. doi:10.1016/j.compstruct.2005.01.018.

[2] Hadi, M., Li, J. External reinforcement of high strength concrete columns. Composite structures, 2004; 65: 279-287. doi:10.1016/j.compstruct.2003.11.003.

[3] Hadi, M. N., Pham, T. M., Lei, X. New method of strengthening reinforced concrete square columns by circularizing and wrapping with fiber-reinforced polymer or steel straps. Journal of Composites for Construction, 2013; 17: 229-238. doi:10.1061/(ASCE)CC.1943-5614.000033.

[4] Hadi, M. N., Widiarsa, I. B. R. Axial and flexural performance of square RC columns wrapped with CFRP under eccentric loading. Journal of Composites for Construction, 2012; 16: 640-649. doi:10.1061/(ASCE)CC.1943-5614.0000301.

[5] Mirmiran, A., Shahawy, M., Samaan, M., Echary, H. E., Mastrapa, J. C., Pico, O. Effect of column parameters on FRP-confined concrete. Journal of Composites for Construction, 1998; 2: 175-185. doi:10.1061/(ASCE)1090-0268(1998)2:4(175.

[6] Pham, T. M., Doan, L. V., Hadi, M. N. Strengthening square reinforced concrete columns by circularisation and FRP confinement. Construction and Building Materials, 2013; 49: 490-499. doi:10.1016/j.conbuildmat.2013.08.082.

[7] Pham, T. M., Hadi, M. N. Confinement model for FRP confined normal-and high-strength concrete circular columns. Construction and Building Materials, 2014; 69: 83-90. doi:10.1016/j.conbuildmat.2014.06.036.

[8] Mandal, S., Hoskin, A., Fam, A. Influence of concrete strength on confinement effectiveness of fiber-reinforced polymer circular jackets. ACI Structural Journal, 2005; 102: 383. doi:10.14359/14409.

[9] Cui, C., Sheikh, S. Analytical model for circular normal-and high-strength concrete columns confined with FRP. Journal of Composites for Construction, 2010; 14: 562-572. doi:10.1061/(ASCE)CC.1943-5614.000011.

[10] Berthet, J., Ferrier, E., Hamelin, P. Compressive behavior of concrete externally confined by composite jackets: Part B: Modeling. Construction and Building Materials, 2006; 20: 338-347. doi:10.1016/j.conbuildmat.2005.01.029.

[11] Xiao, Q., Teng, J., Yu, T. Behavior and modeling of confined high-strength concrete. Journal of Composites for Construction, 2010; 14: 249-259. doi:10.1061/(ASCE)CC.1943-5614.000007.

[12] Girgin, Z. C. Modified Johnston failure criterion from rock mechanics to predict the ultimate strength of fiber reinforced polymer (FRP) confined columns. Polymers, 2013; 6: 59-75. doi:10.3390/polym6010059.

[13] Raza, A., Khan, Q. u. Z., Ahmad, A. Prediction of axial compressive strength for FRP-confined concrete compression members. KSCE Journal of Civil Engineering, 2020; 24: 2099-2109. doi:10.1007/s12205-020-1682-x.

[14] Farzinpour, A., Dehcheshmeh, E. M., Broujerdian, V., Esfahani, S. N., Gandomi, A. H. Efficient boosting-based algorithms for shear strength prediction of squat RC walls. Case Studies in Construction Materials, 2023; 18: e01928. doi:10.1016/j.cscm.2023.e01928.

[15] Naderpour, H., Kheyroddin, A., Amiri, G. G. Prediction of FRP-confined compressive strength of concrete using artificial neural networks. Composite structures, 2010; 92: 2817-2829. doi:10.1016/j.compstruct.2010.04.008.

[16] Elsanadedy, H., Al-Salloum, Y., Abbas, H., Alsayed, S. Prediction of strength parameters of FRP-confined concrete. Composites Part B: Engineering, 2012; 43: 228-239. doi:10.1016/j.compositesb.2011.08.043.

[17] Kumutha, R., Vaidyanathan, R., Palanichamy, M. Behaviour of reinforced concrete rectangular columns strengthened using GFRP. Cement and Concrete Composites, 2007; 29: 609-615. doi:10.1016/j.cemconcomp.2007.03.009.

[18] Koodiani, H. K., Erfanian, N., Majlesi, A., Hosseinzadeh, A., Jafari, E., Shahin, M., Matamoros, A. Calibrating equations to predict the compressive strength of FRP-confined columns using optimized neural network model. Structures, 2023; 56: 105060. doi:10.1016/j.istruc.2023.105060.

[19] Ali, S., Ahmad, J., Iqbal, U., Khan, S., Hadi, M. N. Neural network-based models versus empirical models for the prediction of axial load-carrying capacities of FRP-reinforced circular concrete columns. Structural Concrete, 2023; doi:10.1002/suco.202300420.

[20] Liang, Z., Ramakrishnan, K. R., Ching-Tai, N., Zhang, Z., Fu, J. Vibration-based prediction of residual fatigue life for composite laminates through frequency measurements. Composite structures, 2024; 329: 117771. doi:10.1016/j.compstruct.2023.117771.

[21] Rasouli, M., Broujerdian, V., Kazemnadi, A. Predicting the compressive stress–strain curve of FRP-confined concrete column considering the variation of Poisson's ratio. International Journal of Civil Engineering, 2020; 18: 1365-1380. doi:10.1007/s40999-020-00550-3.

[22] Ke, Y., Zhang, S., Jedrzejko, M., Lin, G., Li, W., Nie, X. Strength models of near-surface mounted (NSM) fibre-reinforced polymer (FRP) shear-strengthened RC beams based on machine learning approaches. Composite structures, 2024; 337: 118045. doi:10.1016/j.compstruct.2024.118045.

[23] Richart, F. E., Brandtzæg, A., Brown, R. L. A study of the failure of concrete under combined compressive stresses. University of Illinois. Engineering Experiment Station. Bulletin; no. 185, 1928;

[24] Mander, J. B., Priestley, M. J., Park, R. Theoretical stress-strain model for confined concrete. Journal of structural engineering, 1988; 114: 1804-1826. doi:10.1061/(ASCE)0733-9445(1988)114:8(1804.

[25] Samaan, M., Mirmiran, A., Shahawy, M. Model of concrete confined by fiber composites. Journal of structural engineering, 1998; 124: 1025-1031. doi:10.1061/(ASCE)0733-9445(1998)124:9(1025.

[26] Razvi, S., Saatcioglu, M. Confinement model for high-strength concrete. Journal of structural engineering, 1999; 125: 281-289. doi:10.1061/(ASCE)0733-9445(1999)125:3(281).

[27] Toutanji, H. Stress-strain characteristics of concrete columns externally confined with advanced fiber composite sheets. ACI Materials Journal, 1999; 96: 397-404. doi:10.14359/639.

[28] Spoelstra, M. R., Monti, G. FRP-confined concrete model. Journal of Composites for Construction, 1999; 3: 143-150. doi:10.1061/(ASCE)1090-0268(1999)3:3(143.

[29] Saafi, M., Toutanji, H., Li, Z. Behavior of concrete columns confined with fiber reinforced polymer tubes. ACI Materials Journal, 1999; 96: 500-509. doi:10.14359/652.

[30] Shehata, I. A., Carneiro, L. A., Shehata, L. C. Strength of short concrete columns confined with CFRP sheets. Materials and structures, 2002; 35: 50-58. doi:10.1007/BF02482090.

[31] Lam, L., Teng, J. G. Design-oriented stress–strain model for FRP-confined concrete. Construction and Building Materials, 2003; 17: 471-489. doi:10.1016/S0950-0618(03)00045-X.

[32] Campione, G., Miraglia, N. Strength and strain capacities of concrete compression members reinforced with FRP. Cement and Concrete Composites, 2003; 25: 31-41. doi:10.1016/S0958-9465(01)00048-8.

[33] Matthys, S., Toutanji, H., Taerwe, L. Stress–strain behavior of large-scale circular columns confined with FRP composites. Journal of structural engineering, 2006; 132: 123-133. doi:10.1061/(ASCE)0733-9445(2006)132:1(12.

[34] Wu, H.-L., Wang, Y.-F., Yu, L., Li, X.-R. Experimental and computational studies on high-strength concrete circular columns confined by aramid fiber-reinforced polymer sheets. Journal of Composites for Construction, 2009; 13: 125-134. doi:10.1061/(ASCE)1090-0268(2009)13:2(125).

[35] Wu, Y.-F., Zhou, Y.-W. Unified strength model based on Hoek-Brown failure criterion for circular and square concrete columns confined by FRP. Journal of Composites for Construction, 2010; 14: 175-184. doi:10.1061/(ASCE)CC.1943-5614.0000062.

[36] Yazici, V., Hadi, M. N. Normalized confinement stiffness approach for modeling FRP-confined concrete. Journal of Composites for Construction, 2012; 16: 520-528. doi:10.1061/(ASCE)CC.1943-5614.0000283.

[37] Chicco, D., Warrens, M. J., Jurman, G. The coefficient of determination R-squared is more informative than SMAPE, MAE, MAPE, MSE and RMSE in regression analysis evaluation. Peerj computer science, 2021; 7: e623. doi:10.7717/peerj-cs.623.

[38] Di Bucchianico, A. Coefficient of Determination (R^2). 1st ed. Hoboken (NJ): John Wiley & Sons; 2007. doi:10.1002/9780470061572.eqr173.